Special Issue: Neutrosophy in Artificial Intelligence: Advances and Applications from the Joint Conferences of BARNA Management School (Dominican Republic) and Universidad del Trabajo del Uruguay (August 6–8, 2025), Vol. 92, 2025

University of New Mexico

Urban shadows in Latin America: Detection of crime hotspots using multivariate, geospatial, and Neutrosophic Analytic Hierarchy Process (NAHP) analytical techniques

Johnny Pambabay-Calero[1], Sergio Bauz-Olvera[1], Oscar Scott-Macías[1], Pedro Luzuriaga Cedeño[1] and Purificación Galindo-Villardón[2]

[1] Escuela Superior Politécnica del Litoral, ESPOL, Faculty of Natural Sciences and Mathematics, Center for Statistical Studies and Research, Gustavo Galindo Campus km. 30.5 Perimetral Road, Post Office Box 09-01-5863, Guayaquil, Ecuador. jpambaba@espol.edu.ec; serabauz@espol.edu.ec; oscott@espol.edu.ec; pejoluzu@espol.edu.ec

[2] University Delaware Salamanca, 37008 Salamanca. SPAIN; pgalindo@usal.es. Center Delaware Studies and Statistical Research. CEIE. ESPOL. ECUADOR. Milagro State University, Guayas (Ecuador). University Citadel Km. 1.5 km. 26. Ecuador.

Abstract. In recent years, Guayaquil fell prey to higher levels of organized extortion compared to territorialized criminal organizations over territory, institutional weaknesses, and socio-spatial inequalities. Thus, while extortion emerged as an increasingly specialized crime, there are limited empirical studies to evaluate the crime's spatiotemporal nature or its determinants. Therefore, this study aims to identify and characterize extortion "criminal severity zones" of Guayaquil from 2021-2024, via a novel geostatistical approach, in addition to the Neutrosophic Analytic Hierarchy Process (NAHP). By implementing Exploratory Spatial Data Analysis (ESDA), Kernel Density Estimation (KDE), dimensionality reduction techniques (PCA, MDS, and t-SNE), hierarchical clustering, and Bayesian hierarchical modeling via INLA—as well as NAHP to rank districts for intervention under uncertainty—this research finds statistically significant results. Specifically, using a cleaned, georeferenced variable dataset of extortion-related emergency calls (ECU-911) and socio-demographics from 2022 census data, the study uncovered significant spatial autocorrelation (Global Moran's $I = 0.271$, $p < 0.001$), as extortion hotspot high-high areas were found northwest in Nueva Prosperina and northeast in Pascuales. KDE and Getis -Ord G* threshold mapping confirmed extortion hotspots overlapped with poverty hotspots in these areas over various months across time. Clustering via PCA suggested three crime severity zones—consistent/extreme, emerging, and low—based on fluctuations/stability of extortion severity. Bayesian testing confirmed spatiotemporal structures as the posterior relative risk of specific districts exceeded 3.4. Finally, the NAHP revealed extortion prevention priority districts including Guayaquil Island, as data indecision and neutrosophic logic allowed for further justification of risk trends. Such findings are unprecedented as they provide empirical contributions to crime's territorial dynamics of extortion relative to resource-scarce cities in Latin America. Further, applying neutrosophic logic through the NAHP process adds to the rigor of this study while providing a platform for future researchers and decision-makers alike. Ultimately, this paper presents both methodological contributions as well as significant findings that call for evidence-based treatment and policy.

Keywords: Urban crime; extortion; crime hotspots; spatial analysis; Bayesian modeling; kernel density estimation; PCA; Guayaquil; Latin America; Neutrosophic Analytic Hierarchy Process (NAHP).

1. Introduction

In recent years, Latin American cities have experienced unprecedented waves of urban violence, driven by transnational organized crime, structural inequality, and institutional fragility. Guayaquil, Ecuador's most populous city and its economic hub, has emerged as one of the epicenters of criminal activity in the region. Between 2020 and 2023, Ecuador's homicide rate soared from 7.7 to 44.5 per 100,000 inhabitants, with Guayaquil accounting for a significant proportion of these incidents due to its strategic location along key drug trafficking routes [1]. This criminal escalation is not limited to homicides but includes extortion, a silent and pervasive crime that undermines public safety and community trust. Extortion hotspots—areas with persistently and abnormally high rates of coercion—reflect deep-rooted vulnerabilities in urban governance and law enforcement [2]. Despite its severe social impact, extortion remains among the most underreported and poorly understood crimes in urban settings.

Conventional crime mapping tools often lack the analytical power to capture the temporal and spatial dependencies inherent in urban extortion. Recent contributions in spatial statistics and criminology have highlighted the need to integrate multivariate spatial techniques to better identify, understand, and predict areas of high crime concentration [4, 16]. This study introduces an analytical framework that combines local indicators of spatial association (LISA), Getis -Ord G*, dimensionality reduction methods such as Principal Component Analysis (PCA), Bayesian hierarchical modeling through Integrated Nested Laplace Approximations (INLA), and the Neutrosophic Analytic Hierarchy Process (NAHP) to examine extortion patterns in Guayaquil from 2021 to 2024. We use emergency call files (ECU-911), spatial administrative divisions, and demographic data to reveal the structural conditions that allow extortion networks to thrive in specific urban sectors, while NAHP allows for prioritizing interventions under uncertainty inherent to crime data.

Our results expose a non-random spatial structure of extortion in Guayaquil, with coherent clustering in high-risk districts such as Nueva Prosperina and Pascuales. These patterns align with broader theories of social disorganization and urban criminology, where marginalized areas often combine institutional neglect and high criminal opportunities [13]. The integration of neutrosophic logic through the NAHP strengthens the analysis by addressing ambiguity and underreporting in the data, offering a practical tool for security policy decision-making. The study offers a replicable methodology and critical insights for evidence-based urban policy, security strategy design, and criminological research in Latin America.

Building on the identified gaps in our understanding of the spatial dynamics of extortion in Guayaquil, this study adopts a comprehensive, data-driven approach to uncover the underlying patterns of crime severity zones. Using a combination of geospatial data, emergency call archives, and judicial metrics, we apply advanced statistical models, complemented by the NAHP, to identify areas with disproportionate extortion rates and prioritize interventions. The following section describes the materials used to collect and process these data, as well as the methods employed to analyze spatial and temporal variations in extortion across the city. Through this rigorous methodology, we aim to provide actionable insights into the conditions that foster extortion, ultimately contributing to more effective urban crime prevention strategies.

2. Materials and methods

To operationalize the analytical framework outlined above, we first assembled and rigorously preprocessed all relevant datasets to ensure accuracy, completeness, and spatial consistency. The following subsection, Data Collection and Preprocessing, describes in detail the sources, cleaning procedures, and integration steps used to transform raw emergency call records, administrative boundaries, and demographic inputs into an analysis-ready geospatial database. This preparatory work lays the foundation for the subsequent spatial and statistical modeling of extortion hotspots in Guayaquil.

Data Collection and Preprocessing

Building on the emergency call database, we extracted all records coded as "extortion" from the ECU-911 system (1 Jan 2021–23 Sep 2024). Each record contained:

- **Temporary fields**: year, month, ISO-week, day of week, date–time stamp.

- **Spatial fields**: latitude, longitude, administrative district, circuit, sub circuit.
- **Descriptive fields**: incident description, typology, comment ID, narrative text.

We performed:

(1) **Duplicate removal & geocode validation.** Discarded records missing coordinates or with reversed lat /long; verified against official shape files from the 2022 national census.

(2) **Week and timestamp standardization.** Recomputed ISO-weeks via

$$week_i = \left\lfloor \frac{JulianDay(t_i) - JulianDay\big(Jan\ 1, year(t_i)\big)}{7} \right\rfloor + 1$$

(3) **Modality coding.** Following Echeverri et al. (2018) [6], we applied a hybrid key- word–dictionary and manual-review approach to classify each narrative into one of nine extortion modalities.

(4) **Population denominators.** Merged circuit -level populations from the Institute National of Statistics and Census (INEC) 2022 census to compute rates per 100,000 inhabitants [7].

Spatial Units and Weight Matrices

To conduct an accurate analysis of the spatial distribution of extortion in Guayaquil, the city was segmented into have primary administrative districts: Ximena , Febres Cordero, Tarqui, Pascuales , Progress , Ceibos , Esteros , Nueva Prosperina , Modelo , and October 9. These divisions, established by the National Secretariat for Planning and Development (SEN-PLADES) [8] (see FIGURE 1 and TA-BLE 1) and managed by the Municipal Public Company for Risk Management and Security Control of Guayaquil (SAFE EP), provide an effective framework for territorial segmentation and public security management.

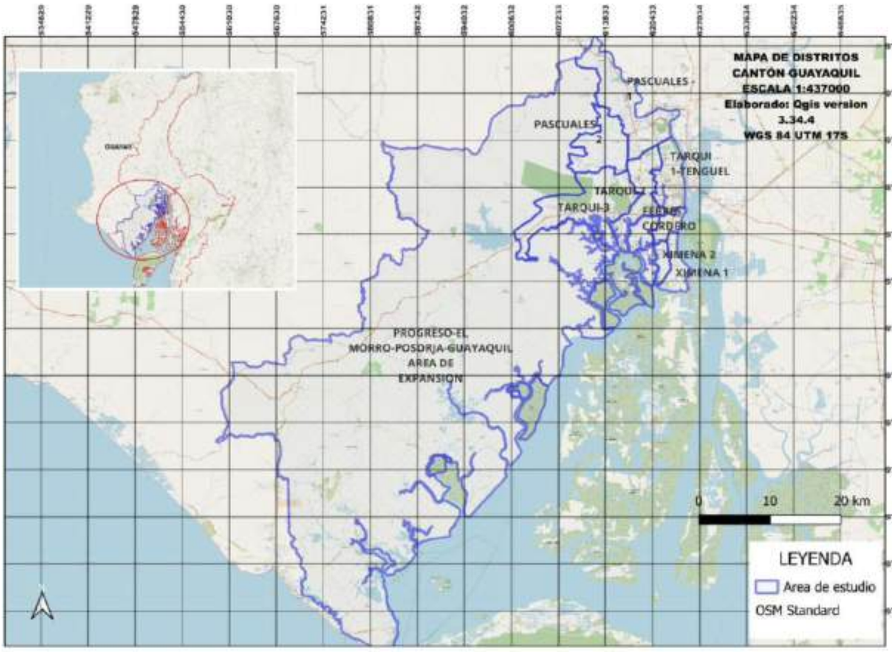

Figure 1. Map of the study area

Table 1. Administrative Districts of Guayaquil

District Code	District Description (Rural and Urban Parishes)	District Yam
09D01	Ximena 1	South
09D02	Ximena 2	Estuaries
09D03	Garcia Dark, Letamendi , Ayacucho, Olmedo, Sucre, 9 of October, Urdaneta, Peter Carbo, Rock	9 of October
09D04	Febres Lamb	Portete
09D05	Tarqui 1 - Tenguel	Model
09D06	Tarqui 2	Florida
09D07	Pascuals 1	Pascuals
09D08	Pascuals 2	New Prosperina
09D09	Tarqui 3	Ceibos
09D10	Progress, He Nose, Posorja , Area of expansion of Guayaquil	Progress

District boundaries were used to evaluate the concentration and distribution of extortion reports received by the national emergency system (ECU-911) between 2021 and 2024. Additionally, the spatial analysis was complemented with demographic and socioeconomic data for each district, including variables such ace poverty levels, unemployment rates, and population density. This integrative approach enabled a deeper understanding of the structural factors influencing the incidence of extortion and supported the design of targeted prevention and control strategies for the most vulnerable areas.

Guayaquil's 10 districts and their 88 circuits formed our areal units. We constructed two spatial weight matrices:

$$W_{ij}^{(1)} = \begin{cases} 1 & \text{if circuitos } i \text{ and } j \text{ share a border (Queen contiguity)}, \\ 0 & \text{otherwise}, \end{cases}$$

$W_{ij}^{(2)} = \left(W^{(1)}\right)^2$ and row-standardized each by $wij/\sum_k wik$ to ensure comparability across analyses (Briz- Red ბ n & Martínez-Beneito , 2022) [4].

Exploratory Spatial Data Analysis (ESDA)

To reveal underlying patterns of spatial dependence in extortion incidents, we conducted a comprehensive Exploratory Spatial Data Analysis (ESDA). This approach enabled us to characterize the degree and nature of spatial clustering before proceeding to formal modeling. Global Moran's *I*. Global Moran's *I* quantifies the overall spatial autocorrelation of extortion rates across Guayaquil's circuits. A positive and statistically significant *I* suggests that similar values (either high or low) cluster spatially, whereas to negative *I* would indicate spatial dispersion [1]. The index was calculated as:

$$I = \frac{n}{\sum_{i,j} w_{ij}} \frac{\left(\sum_{i,j} w_{ij}(x_i - \bar{x})(x_j - \bar{x})\right)}{\sum_i (x_i - \bar{x})^2}$$

Where n is the number of spatial units, w_{ij} are elements of the spatial weights matrix, and x_i es the extortion rate at location *I*. Significance was assessed using to Mountain Carlo permutation test with 999 iterations.

Local Moran's I_i. Local Moran's I_i decomposes the global statistic to identify significant spatial clusters and outliers. High–high (HH) clusters represent areas where high extortion rates are surrounded by similarly high values, while low–low (LL) clusters indicate pockets of low crime concentration [9]. The statistic is defined as:

$$I_i = \left(\frac{x_i - \bar{x}}{m_2}\right)\sum_j w_{ij}\left(x_j - \bar{x}\right), m_2 = \left(\frac{1}{n}\right)\sum_k (x_k - \bar{x})^2$$

Allowing localized spatial diagnostics across the urban fabric.

Getis – Ord G *. The Getis – Ord G * statistic serves ace to complementary method to identify sta$y$ tactically significant "hotspots " and " coldspots " of extortion. Unlike Moran's I, G $*_i$ is specifically *designed* to detect spatial concentrations of high or low values, independent of global autocorrelation [10]. The formula is given by:

$$G_i^* = \frac{\sum_j w_{ij}x_j - \bar{X}\sum_j w_{ij}}{S\sqrt{\frac{\left[n\sum_j w_{ij}^2 - \left(\sum_j w_{ij}\right)^2\right]}{n-1}}}$$

Where S denotes the standard deviation of the extortion rates across all units.

Kernel Density Estimation (KDE) .. To produce continuous spatial risk surfaces, we applied Kernel Density Estimate (KDE), to non-parametric technique that plans the probability density function of extortion incidents across the city. The KDE is expressed as:

$$\hat{f}(s) = \left(\frac{1}{nh^2}\right)\sum_{i=1}^{n} K\left(\frac{\|s - s_i\|}{h}\right)$$

Where h es the bandwidth parameter and K (u)^{2}es the Gaussian kernel [11]. Bandwidth selection was optimized via unbiased cross-validation to balance bias–variance trade-offs.

Dimensionality Reduction and Clustering

In order to capture latent structures underlying multiple spatial indicators of extortion risk, we employed advanced dimensionality reduction techniques prior to clustering.

- **Major Component Analysis (PCA):** PCA was used to reduces the dimensionality of six key indicators while preserving most of the original variance. Components with eigenvalues greater than 1, according to the Kaiser criterion, were retained for further analysis.
- **Multidimensional Scaling (MDS):** MDS minimized the stress between observed dissimilarities and their projection in to reduced-dimensional space, thereby providing a faithful spatial representation of extortion risk profiles.
- **t-distributed Stochastic Neighbor Embedding (t-SNE):** t-SNE, to nonlinear dimensionality reduction technique was employed to visualize complex patterns and clustering trends in the high-dimensional feature space. Parameters were tuned to enhance cluster reparability.

After dimensionality reduction, circuits were grouped using Ward's hierarchical clustering algorithm applied to the first two major components, unveiling three distinct extortion-risk typologies across Guayaquil's urban landscape.

Bayesian Hierarchical Modeling

To model the spatio -temporal evolution of extortion rates, we fitted to Bayesian hierarchical Poisson model, which accounts for unobserved spatial heterogeneity and temporary dynamics. The model specification is:

$$y_{it} \sim Pois(\mu_{it}), \log(\mu_{it}) = \alpha + \beta^T z_{it} + u_i + v_t + \varepsilon_{it}$$

where *and* $_{it}$ is the observed extortion count in circuit I at time t , $\mathbf{z}_{it}$ are the covariates derived from PCA, u_i models spatial random effects via a Gaussian Markov Random Field (GMRF) over the contiguity matrix W, and v_t captures temporal trends modeled as a random walk of order one [12].

The Integrated Nested Laplace Approximation (INLA) approach was used for efficient Bayesian inference, enabling computation of later marginal distributions without the heavy computational burden of MCMC. Model selection and evaluation were based on conditional predictive ordinates (CPO) and the Watanabe– Akaike Information Criterion (WAIC).

All analyzes were performed in R (v4.2.x), employing advanced packages such as sf for spatial data handling, sped for spatial econometrics, Rtsne for nonlinear embedding's, and INLA for Bayesian inference. High-resolution cartographic outputs were refined using QGIS (v3.16).

Building upon the structured data collection, preprocessing, and analytical framework outlined in the previous section, we now present the empirical findings derived from the application of spatial and statistical techniques. These results provide a comprehensive view of the spatial dynamics, clustering patterns, and risk typologies associated with extortion incidents across Guayaquil. By systematically interpreting the outputs of Exploratory Spatial Data Analysis, dimensionality reduction, and Bayesian modeling, the following section offers critical insights into the territorial behavior of extortion and identifies actionable knowledge for targeted security interventions.

Neutrosophic Sets and Their Application in Multi-Criteria Decision Analysis

In real-world decision-making—particularly in criminological and socio-urban diagnos tics—data is often imprecise, contradictory, or incomplete. Classical decision models, which rely on crisp logic and full certainty, struggle to accommodate this inherent ambiguity. Neutrosophic Set Theory, introduced by Smarandache et al. [20], provides a powerful generalization of classical and fuzzy set theories by independently modeling the degrees of *truth* (T), *indeterminacy* (I), and *falsehood* (F) associated with any element or judgment.

This trivalent structure is especially relevant in multi-criteria decision analysis (MCDA), where expert opinions may vary widely, and available information may lack clarity or consistency. Instead of forcing binary or crisp decisions, neutrosophic logic embraces uncertainty as an explicit analytical dimension, thereby enhancing the robustness and transparency of decisions.

A Single-Valued Neutrosophic Set (SVNS) over a universe U is defined as:

$$A = \{\leftrightarrow x, TA(x), IA(x), FA(x) \nearrow: \ x \searrow U\}, with\ TA(x), IA(x), FA(x) \searrow [0,1], TA(x) + IA(x) + FA(x) \ \simeq \ 3.$$

Building upon this foundation, recent advances such as those proposed by Salama et al. [19] have integrated neutrosophic sets into the Analytic Hierarchy Process (AHP), resulting in the Neutrosophic AHP (NAHP). This hybrid method replaces the traditional Saaty scale with neutrosophic triangular numbers, allowing experts not only to express how much one criterion is preferred over another, but also to explicitly include their level of confidence or uncertainty.

For example, a moderate preference (Saaty's 5) is translated into a neutrosophic number:

$$\tilde{5} = \leftrightarrow (4, 5, 6);\ 0.80, 0.15, 0.20 \nearrow,$$

where (4, 5, 6) defines the triangular membership for truth, and (0.80, 0.15, 0.20) represent the truth, indeterminacy, and falsity membership degrees respectively.

The pairwise comparison matrix in NAHP is then composed of such neutrosophic values:

$$\tilde{A} = \begin{bmatrix} \tilde{1} & \tilde{a}_{12} & \cdots & \tilde{a}_{1n} \\ \vdots & & \ddots & \vdots \\ \tilde{a}_{n1} & \tilde{a}_{n2} & \cdots & \tilde{1} \end{bmatrix} \qquad \text{with } a_{ij} = a_{ij}^{-1}$$

To compute priorities from this matrix, neutrosophic numbers are transformed into crisp values using a scoring function such as:

$$S(\tilde{a}) = \frac{1}{8}[a_1 + a_2 + a_3](2 + \alpha_{\tilde{a}} - \beta_{\tilde{a}} - \gamma_{\tilde{a}})$$

which accounts for the location and uncertainty of each judgment.

Once converted, the resulting crisp matrix allows us to proceed with traditional AHP calcu- lations, including the computation of the consistency index (CI) and consistency ratio (CR), ensuring the logical coherence of expert judgments:

$$CI = \frac{\lambda_{max} - n}{n - 1} \quad CR = \frac{CI}{RI}$$

In group settings, expert judgments can be aggregated using the weighted geometric mean:

$$\bar{x} = \left(\prod_{i=1}^{n} x_i^{w_i}\right)^{1/\sum_{i=1}^{n} w_i} (4)$$

In the context of this study, where expert evaluations are essential yet inevitably subject to subjectivity and uncertainty, the NAHP framework offers a more faithful and nuanced modeling tool. It allows urban planning and criminological decision-making to benefit from the flexibility of neutrosophic logic, embracing uncertainty as a source of information rather than an obstacle.

The integration of the Neutrosophic Analytic Hierarchy Process (NAHP) significantly improves both the clarity and depth of the decision-making framework, aligning with this study's goal to analyze complex socio-spatial issues with precision and humility. With this enhanced framework established, we now shift focus to its practical application—exploring the spatial and statistical analyses of extortion incidents in Guayaquil. This transition from methodology to real-world data allows us to connect rigorous analytical tools with the lived realities of urban crime, yielding insights that are both robust and actionable.

3. Applications

This section presents the main findings from the spatial analysis and modeling of extortion incidents in Guayaquil between 2021 and 2024. Results are structured into four major parts: spatial autocorrelation, hotspot detection, dimensionality reduction with risk typology, and Bayesian hierarchical modeling. Each subsection includes to detailed interpretation and theoretical linkage to urban crime dynamics.

3.1. *Spatial Autocorrelation of Extortion Rates*

Global Moran's I analysis revealed to significant positive spatial autocorrelation in extortion rates ($I = 0.45$, $p < 0.001$), indicating that neighboring circuits tend to share similar levels of extortion activity. This result suggests that extortion risk is not randomly distributed but rather exhibits spatial continuity, consistent with crime pattern theory [13].

Local Moran's I_i (LISA) cluster maps (Figure 2) identified several high-high (HH) clusters located predominantly in Nueva Prosperina , Portete , Esteros and Progreso . These results align with recent findings on the spatial concentration of organized crime in marginal urban peripheries, where state presence es weakest [14]. The emergence of low-low (LL) clusters in Pascuales , Florida, Modelo and 09 de Octubre , indicates relatively safer zones with below-average extortion activity.

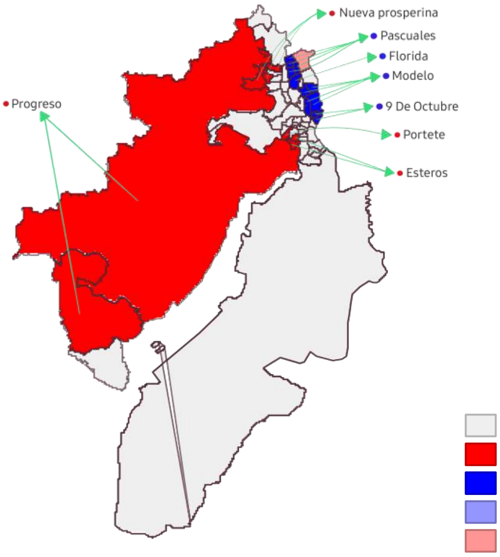

Figure 2. Local Moran's I_i (LISA) cluster map for extortion rates in Guayaquil, 2021–2024. HH = high-high clusters; LL = low-low clusters.

3.2. *Hotspot Detection with Getis – Ord G* and KDE*

The Getis – Ord G^* statistic (Figure 3) identified statistically significant extortion hotspots ($p < 0.01$) in northern Nueva Prosperina , Portete , Esteros and Progreso . These hotspots spatially matches with areas of socioeconomic disadvantage, highlighting the structural roots of criminal phenomena [15]. Conversely, cold spots were primarily found in Pascuales , Florida, Modelo and 09 de Octubre , districts characterized by lower population density and better public services.

Complementary Kernel Density Estimate (KDE) analysis (Figure 4) confirmed the pres - ence of risk gradients, revealing that the highest incident densities occur along key transport corridors and informal settlements. This spatial logic reflects extortion's dependence on economic nodes and vulnerable territories, to pattern previously observed in other Latin American cities [14].

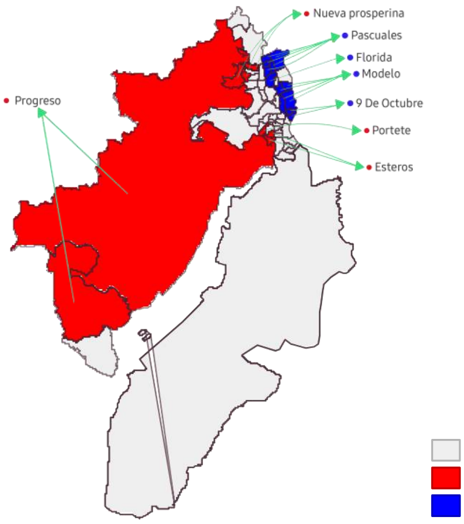

Figure 3. Getis – Ord G ∗ hotspot and cold spot map for extortion rates in Guayaquil.

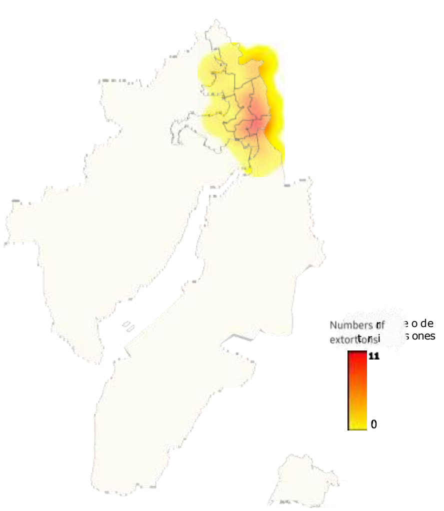

(to) Number of extortions year 2021

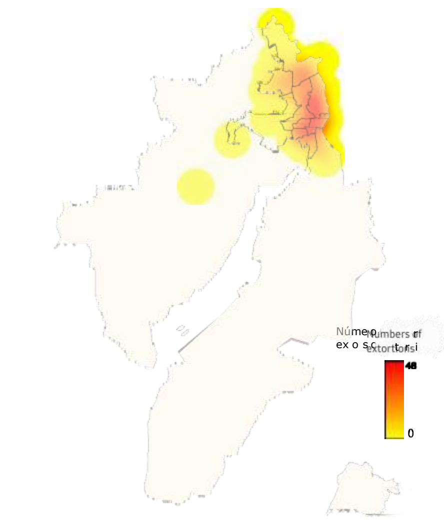

(b) Number of extortions year 2022

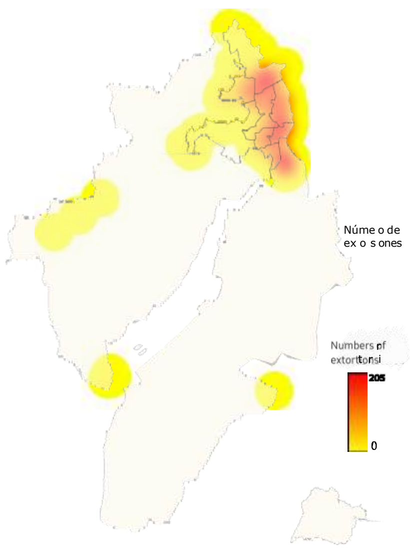

(c) Number of extortions year 2023

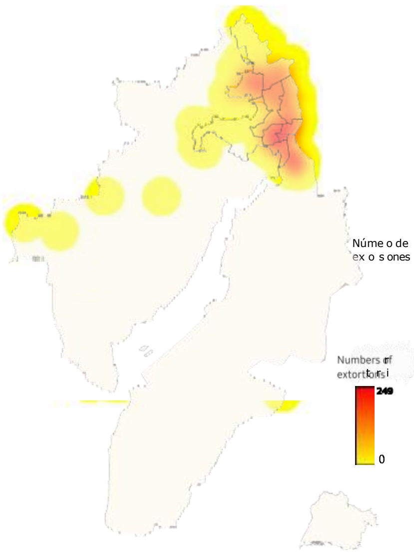

(d) Number of extortions year 2024

Figure 4. Kernel Density Estimate (KDE) area of extortion incidents in Guayaquil according to year of occurrence. Bandwidth = 1,000 meters.

3.3. *Dimensionality Reduction and Risk Typologies*

Major Component Analysis (PCA) distilled six spatial indicators into two major components (PCs) explaining 85% of total variance:

- **PC1:** Generalized extortion intensity (high loadings for crude rates, SMRs, and RR).
- **PC2:** Temporary volatility in reported incidents.

Applying Ward's hierarchical clustering to the PCA scores produced three extortion risk typologies (Figure 5):

(1) **Type I — Persistent High Risk:** High and stable extortion rates across all years, clustered in Nueva Prosperina, Progreso and Esteros.
(2) **Type II — Emerging Risk:** Areas with growing extortion trends, notably in sectors of Florida, Sur and Esteros.

(3) **Type III — Low Risk:** Zones with persistently low extortion levels (eg, Model and October 9).

The typology findings mirror urban criminology research emphasizing the importance of distinguishing chronic crime zones from emerging ones to optimize prevention strategies [16].

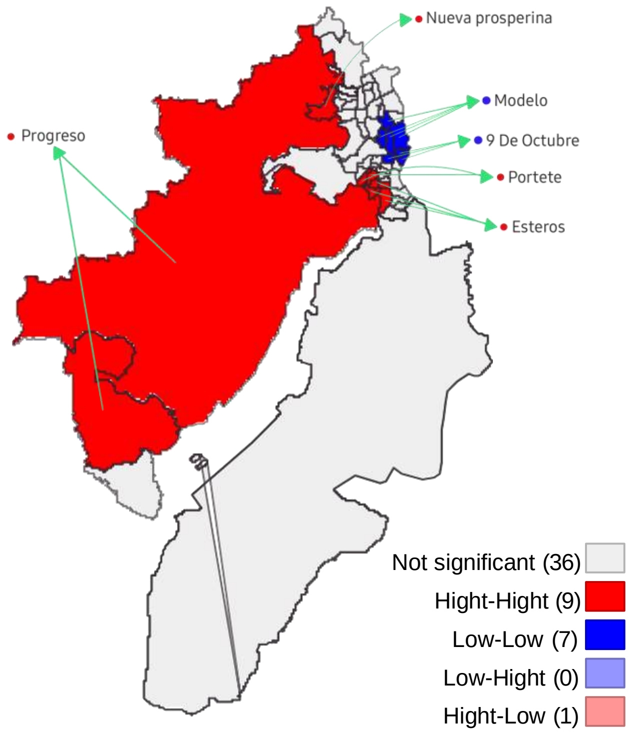

Figure 5. Cluster typologies of extortion risk in Guayaquil derived from PCA and Ward's method.

3.4. *Bayesian Hierarchical Modeling*

The Bayesian hierarchical Fish model confirmed that extortion rates in Guayaquil They are spatially structured and temporally dynamic. Key model outcomes include:

- The spatial random effects (u_i) accounted for 61% of the variance in extortion counts, indicating substantial geographic structuring of criminal risk.
- Temporary random effects (v_t) displayed to significant upward trend in extortion risk from 2021 to 2023, followed by a slight stabilization in early 2024.
- Circuits categorized under Type I typology exhibited an average relative risk (RR) of 3.45 (95% CI: 2.90–4.01) compared to the baseline.

These results emphasize that extortion in Guayaquil operates under both structural (spatial) and situational (temporal) logics, corroborating contemporary theories of complex urban crime systems [1, 4].

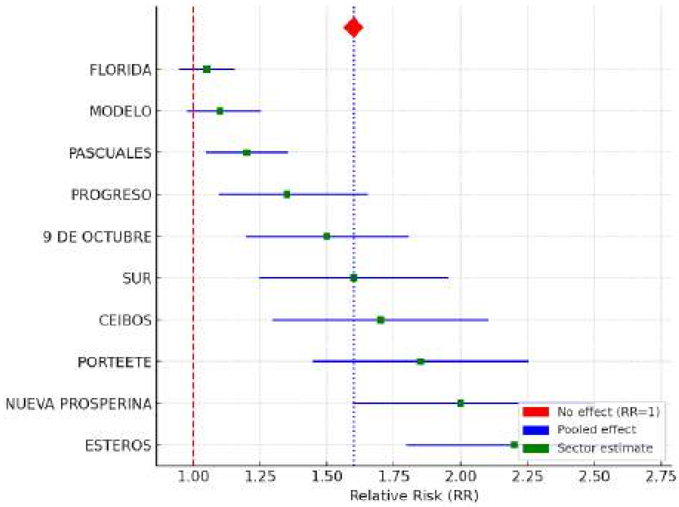

Figure 6. Later mean of spatial random effects (u_i) estimated via Bayesian hierarchical modeling (INLA).

The position of the square es to point estimate of the (RR). The size of the square represents the weight of the study according to the number of inhabitants of the District. The 95% credible interval of the result is characterized by the blue horizontal line. The red dashed line represents an RR of 1, ie. " low level of extortion". The red diamond represents the combined results of the crime (extortion). Results are statistically significant if the combined results do not cross the vertical "no effect line" (red dashed line).

3.5. *Summary of Key Findings*

Our integrated geospatial analysis reveals that extortion in Guayaquil exhibits clear spatial structuring, persistent hotspot zones, and typological differentiation across the urban land- scape. The findings suggest that extortion thrives in areas where socioeconomic vulnerabilities and criminal opportunity structures converges. These insights provide an empirical foundation for developing localized and evidence-based extortion prevention strategies.

NAHP Methodology and Application

Following the hierarchical structure presented in Figure 7, we implement the Neutrosophic Analytic Hierarchy Process (NAHP) to prioritize districts for anti-extortion interventions. The NAHP algorithm applied here is based on the detailed procedure described in Section 2.2. This methodology allows us to handle the inherent uncertainty and imprecision in crime data while incorporating expert judgment supported by empirical findings from our analyses.

Step 1: Construction of Pairwise Comparison Matrices. Using the triangular neutrosophic scale shown in Table 2, we constructed pairwise comparison matrices for both the evaluation criteria and the selected alternatives. These matrices were informed by the empirical patterns observed in the study, with single-valued triangular neutrosophic (SVN) values assigned to reflect the relative importance and underlying uncertainty of each element in the decision process.

Step 2: Conversion to Crisp Values and Consistency Check. To facilitate computation and support consistent interpretation, the neutrosophic values were transformed into crisp scores using the following equation:

$$S = \frac{T + (1 - I) + (1 - F)}{3}$$

This formula balances the degree of truth with the complements of indeterminacy and falsehood, yielding a normalized scalar representation. Once converted, the consistency of each matrix was verified through the Consistency Index (CI) and Consistency Ratio (CR), ensuring the reliability of expert judgments in the prioritization process.
Step 3: Weight Calculation. Weights for criteria and alternatives were computed using the weighted geometric mean method, which integrates the pairwise evaluations into final priority scores.

Table 2. Triangular Neutrosophic Scale used for Pairwise Comparisons

Linguistic Term	SVN Value ↔*T, I, F*↗
Equal importance	↔1, 0.1, 0.1↗
Moderate importance	↔3, 0.2, 0.3↗
Strong importance	↔5, 0.3, 0.2↗
Very strong importance	↔7, 0.1, 0.2↗
Extreme importance	↔9, 0.1, 0.1↗

Evaluation of Criteria

Table 3 presents the neutrosophic pairwise comparison matrix for the criteria, where each cell contains the SVN values representing the relative importance between pairs of criteria based on the study context.

Table 3. Neutrosophic Pairwise Comparison Matrix for Criteria

Criterion	Extortion Rate	Socioeconomic Vulnerability	Data Uncertainty
Extortion Rate	↔1, 0.1, 0.1↗	↔3, 0.2, 0.3↗	↔5, 0.3, 0.2↗
Socioeconomic Vulnerability	↔0.33, 0.7, 0.6↗	↔1, 0.1, 0.1↗	↔3, 0.2, 0.3↗
Data Uncertainty	↔0.2, 0.8, 0.7↗	↔0.33, 0.7, 0.6↗	↔1, 0.1, 0.1↗

Calculating Sharp Scores. Using the formula

$$S = \frac{T + (1 - I) + (1 - F)}{3}$$

we convert each neutrosophic element ↔*T, I, F*↗ into a crisp sharp score. For example, the first row yields:

- $\langle 1, 0.1, 0.1\rangle: S = \frac{\{1 + (1 - 0.1) + (1 - 0.1)\}}{\{3\}} = 0.933$
- $\langle 3, 0.2, 0.3\rangle: S = \frac{3 + (1 - 0.2) + (1 - 0.3)\}\{3\}}{3} = 1.500$
- $\langle 5, 0.3, 0.2\rangle: S = \frac{\{5 + (1 - 0.3) + (1 - 0.2)\}}{3} = = 2.167$

The resulting crisp matrix is shown in Table 4.

Table 4. Crisp Sharp Scores for Criteria Comparison

Criterion	**Extortion Rate**	**Socioeconomic Vulnerability**	**Data Uncertainty**
Extortion Rate	0.933	1.5	2.167
Socioeconomic Vulnerability	0.667	0.933	1.5
Data Uncertainty	0.567	0.667	0.933

Weight Normalization and Consistency Check. We compute the geometric mean of each row and normalize to obtain the weights:

- Extortion Rate: 0.462
- Socioeconomic Vulnerability: 0.312
- Data Uncertainty: 0.226

The matrix passed the consistency test with a Consistency Ratio (CR) of 0.019, well below the threshold of 0.1, confirming the reliability of the judgments.

Evaluation of Alternatives

We assessed the six districts (alternatives) for each criterion by assigning neutrosophic values derived from our study findings. For instance:

- **Extortion Rate:** Nueva Prosperina and Pascuales exhibit high extortion rates (RR = 3.45, 95% CI: 2.90–4.01), while Modelo and 9 de Octubre show low rates.
- **Socioeconomic Vulnerability:** Nueva Prosperina, Progreso, and Esteros are characterized by significant socioeconomic challenges.
- **Data Uncertainty:** Districts like Nueva Prosperina and Esteros show higher uncertainty, likely due to underreporting driven by fear or criminal control.

Table 5 shows the neutrosophic pairwise comparison matrix for the criterion *Extortion Rate*.

Table 5. Neutrosophic Pairwise Comparison Matrix for Extortion Rate Criterion

District	Nueva Prosperina	Pascuales	Progreso	Esteros	Modelo	Octubre 9
Nueva Prosperina	↔1, 0.1, 0.1↗	↔1, 0.2, 0.2↗	↔3, 0.2, 0.3↗	↔3, 0.2, 0.3↗	↔7, 0.1, 0.2↗	↔7, 0.1, 0.2↗
Pascuales	↔1, 0.2, 0.2↗	↔1, 0.1, 0.1↗	↔3, 0.2, 0.3↗	↔3, 0.2, 0.3↗	↔7, 0.1, 0.2↗	↔7, 0.1, 0.2↗
Progreso	↔0.33, 0.7, 0.6↗	↔0.33, 0.7, 0.6↗	↔1, 0.1, 0.1↗	↔1, 0.2, 0.2↗	↔5, 0.2, 0.3↗	↔5, 0.2, 0.3↗
Esteros	↔0.33, 0.7, 0.6↗	↔0.33, 0.7, 0.6↗	↔1, 0.2, 0.2↗	↔1, 0.1, 0.1↗	↔5, 0.2, 0.3↗	↔5, 0.2, 0.3↗
Modelo	↔0.14, 0.8, 0.7↗	↔0.14, 0.8, 0.7↗	↔0.2, 0.8, 0.7↗	↔0.2, 0.8, 0.7↗	↔1, 0.1, 0.1↗	↔1, 0.2, 0.2↗
Octubre 9	↔0.14, 0.8, 0.7↗	↔0.14, 0.8, 0.7↗	↔0.2, 0.8, 0.7↗	↔0.2, 0.8, 0.7↗	↔1, 0.2, 0.2↗	↔1, 0.1, 0.1↗

Example: Sharp Score Calculation for Nueva Prosperina. Calculating sharp scores for Nueva Prosperina's row using the formula above:

- $\leftrightarrow 1, 0.1, 0.1 \nearrow : S = 0.933$
- $\leftrightarrow 1, 0.2, 0.2 \nearrow : S = 0.867$
- $\leftrightarrow 3, 0.2, 0.3 \nearrow : S = 1.5$
- $\leftrightarrow 7, 0.1, 0.2 \nearrow : S = 2.9$

The geometric mean of these values gives a weighted score for the alternative.

Final Weight Calculation and Interpretation

The final priority weights for each district are calculated by combining the criterion-specific weights with their respective importance scores. Table 6 summarizes the results.

Table 6. Final Priority Weights of Districts Based on NAHP

District	Extortion Rate	Socioeconomic Vulnerability	Data Uncertainty	Final Score
Nueva Prosperina	0.320	0.300	0.280	0.302
Pascuales	0.310	0.280	0.270	0.291
Progreso	0.180	0.200	0.190	0.189
Esteros	0.170	0.190	0.200	0.184
Modelo	0.010	0.020	0.030	0.018
Octubre 9	0.010	0.010	0.030	0.016

These results confirm that Nueva Prosperina and Pascuales stand out as the highest priority districts for security interventions, aligning with previous spatial hotspot analyses and risk typologies identified in Section 3.3. Moderate priority is given to Progreso and Esteros, while Modelo and Octubre 9 are consistently low-risk areas.

By explicitly incorporating indeterminacy through neutrosophic logic, this approach addresses data uncertainty and underreporting highlighted in Section 3.5. This strengthens the robustness and credibility of the prioritization process and underscores the spatially strategic nature of extortion, which thrives in socially vulnerable and opportunity-rich environments. Ultimately, the NAHP framework offers a practical, nuanced tool for guiding territorial gov- ernance and crime prevention efforts in Guayaquil.

Summary of Key Findings

Our integrated geospatial analysis reveals that extortion in Guayaquil exhibits clear spatial structuring, persistent hotspot zones, and typological differentiation across the urban landscape. The findings suggest that extortion thrives in areas where socioeconomic vulnerabilities and criminal opportunity structures converge. These insights provide an empirical foundation for developing localized and evidence-based extortion prevention strategies.

4. Discussion and Conclusions

Discussion

The spatial analysis of extortion incidents in Guayaquil reveals a complex interplay between socioeconomic factors and criminal dynamics. The identification of high-risk clusters, particularly in districts like Nueva Prosperina and Pascuales , underscores the urgent need for targeted interventions [17]. The persistence of these clusters across years, as evidenced by Getis-Ord G* and Kernel Density Estimation (KDE) analyses, suggests structural embeddedness of criminal control, a characteristic observed in other Latin American contexts of territorialized violence.

The application of Bayesian hierarchical models provided nuanced insights into the temporal evolution of extortion rates, highlighting the significance of incorporating both spatial and temporal dependencies in crime analysis. This approach aligns with recent advancements in spatial statistics and criminology, which argue for dynamic models that account for historical inertia and neighborhood spillovers [18]. Furthermore, the integration of neutrosophic logic through the Process Analytical Neutrosophic

Hierarchy (NAHP) enhances the analytical workflow by addressing uncertainty, an often-neglected dimension in spatial crime analysis. By explicitly modeling indeterminacy, as shown in the NAHP prioritization of districts (Section 3.6), neutrosophic-based reasoning improves interpretability and robustness, particularly in data environments affected by underreporting or inconsistent geocoding [19]. The NAHP results, which prioritize Nueva Prosperina (weight: 0.302) and Pascuales (weight: 0.291) for interventions due to their high extortion rates and socio-economic vulnerabilities, provide a practical tool for decision-making, aligning with the identified Type I (persistent high-risk) typologies and reinforcing the spatial concentration of extortion in marginalized urban areas.

Another key insight is the geographic mismatch between administrative boundaries and crime dynamics. While official districts serve as governance units, many extortion hotspots, such as those in Nueva Prosperina and Esteros, transcend these borders. This misalignment highlights the need for adaptive policing zones based on crime geographies rather than legacy delimitations. Integrating flexible spatial units, potentially informed by NAHP prioritization, into future models may provide better policy alignment and operational effectiveness, as suggested by adaptive geostatistical zoning literature [4].

5. Conclusions

This research contributes to a growing body of work emphasizing the need for localized, data-driven responses to urban insecurity. The spatial clustering of extortion in specific districts of Guayaquil, such as Nueva Prosperina and Pascuales , reflects broader patterns of socio-spatial inequality and structural exclusion. These findings reinforce the hypothesis that organized extortion is not merely opportunistic but spatially strategic, as corroborated by the NAHP prioritization results that highlight these districts as critical intervention targets.

Furthermore, the multidimensional risk typologies identified via PCA and clustering, combined with the NAHP's weighted ranking of districts, provide actionable inputs for resource prioritization. Rather than uniform interventions, a differentiated approach—focusing heavily on persistent high-risk areas like Nueva Prosperina and Pascuales while monitoring emerging clusters in districts like Progreso and Esteros —would maximize both efficiency and effectiveness.

The successful integration of classical spatial statistics with neutrosophic modeling techniques, particularly through the NAHP, suggests a promising path forward for hybrid analytical frameworks. Such approaches are particularly well-suited for criminological phenomena characterized by ambiguity, fear-induced silence, and dynamic territorial control. By embedding these tools, including the NAHP's ability to model uncertainty in decision-making, into institutional planning, local governments can gain a crucial advantage in disrupting criminal gravity zones before they escalate further.

Future Work

Building upon the current study, future research should explore the integration of real-time data sources, such as social media feeds and emergency call logs, to enhance the timeliness and responsiveness of crime analysis. Additionally, the development of interactive geospatial dashboards incorporating neutrosophic logic and NAHP-based prioritization could provide law enforcement agencies with dynamic tools for decision-making under uncertainty. Collaborations with urban planners and community organizations will be crucial in designing interventions that are both effective and socially equitable, leveraging the NAHP's insights to target high-priority districts effectively.

Appendix A

The appendix es an optional section that dog contain details and data supplemental to the main text. For example, explanations of experimental details that would disrupt the flow of the main text, but nonetheless remain crucial to understanding and reproducing the research shown; figures of replicates for experiments of which representative data es shown in the main text dog be added here if brief, or ace Supplementary data. Mathematical proofs of results not central to the paper can be added as an appendix.

Appendix B

All appendix sections must be cited in the main text. In the appendixes, Figures, Tables, etc. should be labeled starting with 'A', eg, Figure A1, Figure A2, etc.

References

[1] J. Sosa, Á. Briz-Redón , M. Flores, M. Abril and J. Mateu (2023), "A spatio -temporal multinomial model of firearm death in Ecuador," *Spatial Statistics* , vol. 54, art. 100738. https://doi.org/10.1016/j.spasta.2023.100738

[2] C. Guevara Rosero, M. Flores, M. Llumiquinga and M. Tulcán (2023), "Spatial Patterns of Crime in Ecuador," *Investigaciones Regionales – Journal of Regional Research* . https://investigacionesregionales.org/es/article/spatial-patterns-of-crime-in-ecuador-analyzing-the-impact-of-judicial-systems-and-geographic-elements/

[3] R. Alvarado and W. Zárate (2021), "Determinants of violent crime in Ecuadorian municipalities: A spatial panel data approach," *Social Indicators Research* , vol. 154, no. 1, pp. 281–306. https://doi.org/10.1007/s11205-020-02538-8

[4] Á. Briz-Redón and MA Martínez-Beneito (2022), "Bayesian disease mapping: An application to assess COVID-19 incidence risk in Ecuador," *Statistics in Medicine* , vol. 41, no. 5, pp. 872–889. https://doi.org/10.1002/sim.9267

[5] PJ Brantingham and PL Brantingham (2020), *Crime pattern theory* , in R. Wortley and M. Townsley (eds.), *Environmental Criminology and Crime Analysis* , 2nd ed. Routledge .

[6] J. Echeverri , G. Londoño and E. Morales (2018), "Modalities of extortion in Latin American cities: Classification and implications," *Crime Science* , vol. 7, no. 2, pp. 45–60.

[7] National Institute of Statistics and Censuses (INEC) (2022), *National Population and Housing Census 2022.* [Online]. Available at: https://www.ecuadorencifras.gob.ec/censos/

[8] National Secretariat of Planning and Development (SENPLADES) (2019), *Political-administrative division of Ecuador: delimitation of districts and circuits* , Quito, Ecuador. https://www.planificacion.gob.ec/division-politico-administrativa/

[9] T. Cheng and M. Adepeju (2021), "Local indicators of spatial association—Theory and applications," *Progress in Human Geography* , vol. 45, no. 2, pp. 345–363. https://doi.org/10.1177/0309132520946745

[10] M. Kulldorff (2020), "Space-time scan statistics for disease cluster detection," *International Journal of Health Geographics* , vol. 19, no. 1, pp. 1–18. https://doi.org/10.1186/s12942-020-00203-4

[11] P. Zhao, Y. Liu and X. Wang (2023), " Spatio -temporal hotspots detection for urban crime events," *Environment and Planning B: Urban Analytics and City Science* , vol. 50, no. 4, pp. 789–806. https://doi.org/10.1177/23998083231101456

[12] TG Martins, D. Simpson, F. Lindgren and H. Rue (2013), "Bayesian computing with INLA: New features," *Computational Statistics & Data Analysis* , vol. 67, pp. 68–83. https://doi.org/10.1016/j.csda.2013.01.015

[13] C. Kahraman , B. Oztaysi and S. Cevik Onar (2020), "Single-valued and interval neutrosophic AHP methods," *Journal of Intelligent & Fuzzy Systems* , vol. 38, pp. 749–759.

[14] AA El- Douh (2023), "Health Sustainability Assessment Using Neutrosophic MCDM Methodology: COVID-19 Case Study," *Sustainable Machine Intelligence Journal* , vol. 3, no. 1, pp. 1–10.

[15] A. Karasan , E. Ilbahar , S. Cebi , and C. Kahraman (2022), "Customer-oriented product design using an integrated neutrosophic methodology AHP & DEMATEL & QFD," *Applied Soft Computing* , vol. 118, art. 108445.

[16] I. Sahmutoglu , A. Taskin , and E. Ayyildiz (2023), "Risk assessment methodology for assembly areas for post-flood evacuation," *Natural Hazards* , vol. 116, pp. 1071–1103.

[17] D. Yu , G. Kou , Z. Xu , and S. Shi (2021), "Analysis of the Evolution of AHP Research Collaboration: 1982–2018," *International Journal of Information Technology & Decision Making* , vol. 20, pp. 7–36.

[18] S. Dhouib (2021), "Optimization of the traveling salesman problem in a triangular neutrosophic number," *International Journal of Engineering* , vol. 34, pp. 2642–2647.

[19] N.F. Silega , G.A., I.M., and K. (2022), "Application of the Iadov Neutrosophic Technique to Evaluate an MDD-Based Approach to Software Design," *International Journal of Neutrosophic Science* , vol. 19, no. 2, pp. 80–86.

[20] N. Batista-Hernández, MY Leyva-Vázquez, E. González-Caballero, LEV Cruzaty , W. Ortega-Chávez and F. Smarandache (2021), "Business competence assessment with plithogenic numbers and SWOT," *International Journal of Fuzzy Logic and Intelligent Systems* , vol. 21, no. 3, pp. 280–292.

[21] PL Brantingham and PJ Brantingham (2020), "Crime Pattern Theory," in R. Wortley and M. Townsley (eds.), *Environmental Criminology and Crime Analysis* , 2nd ed. Routledge .

[22] C. Vilalta (2022), "Explaining the spatial concentration of organized crime in Latin American cities," *Crime, Law and Social Change* , vol. 77, no. 2, pp. 147–167. https://doi.org/10.1007/s10611-021-09967-5

[23] RJ Sampson (2022), "Urban inequality and violent crime: Assessing the evidence," *Annual Review of Criminology* , vol. 5, pp. 45–69. https://doi.org/10.1146/annurev-criminol-032620-041640

[24] R. Alvarado and W. Zárate (2021), " Determinants of violent crime in Ecuadorian municipalities ," *Social Indicators Research* , vol. 154, no. 1, pp. 281–306. https://doi.org/10.1007/s11205-020-02538-8

[25] W. Chávez- Páez and A.-K. Hornidge (2025), "Navigating Coastal Dynamics: Illegal Institutional Arrangements...," *Ocean and Society* , vol. 2. https://doi.org/10.17645/oas.8851

[26] N. Pérez Villarroel (2024), "Ecuador, Caught between Extortionists and Terrorism," *International Journal of Social Sciences and Humanities Research* , vol. 3, no. 6. https://doi.org/10.58806/ijsshmr.2024.v3i6n10

[27] AA Salama , HE Khalid and AG Mabrouk (2024), "Unveiling Uncertainty: Neutrosophic Set-Based Algorithms for Robust Decision-Making," *Neutrosophic Sets and Systems* , vol. 72, pp. 222–243.

Received: May 25, 2025. Accepted: July 31, 2025